The Korean Journal of Ceramics, **1** [2] 81-85 (1995)

Dielectric Characteristics of $Pb(Sc_{1/2-x}Ta_{1/2+x})O_{3+x}$ Ceramic System

Nam-Kyoung Kim, Dwight D. Viehland* and David A. Payne*

Dept. of Inorg. Mater. Eng., Kyungpook Nat. Univ., Taegu 702-701, Korea
**Dept. of Mater. Sci. and Eng., and Mater. Research Laboratory Univ. of Illinois at Urbana-Champaign, Urbana, Illinois 61801 USA*
(Received February 10, 1995)

PST-series specimens with stoichiometric and nonstoichiometric compositions were prepared and the effects of composition modification on phase formation and dielectric response were investigated. The phases formed on calcination were mainly perovskite and trace amount of pyrochlore(s), with an increase of the latter phase(s) as the composition became more nonstoichiometric. The sintered samples showed thermal hysteresis and diffuseness in phase transition with a small degree of frequency relaxation. Temperatures corresponding to maximum values of dielectric constant and loss were relatively insensitive to the composition change while the maximum values were very sensitive to that.

Key words : Lead scandium tantalate, Perovskite, Phase formation, Thermal hysteresis

I. Introduction

In search of new ferroelectric compounds (between more than two oxide components) with a perovskite structure, $Pb(Sc_{1/2}Ta_{1/2})O_3$ (PST) was first synthesized in the late 50's in Russia.[1] Since then, the PST has been investigated extensively as the PST lies close to the stability boundary between the ordered and disordered state of the B-site cation arrangements.[2,3] In the PST, the ions of Sc^{3+} and Ta^{5+} are located in the octahedral positions of the perovskite structure. The degree of ordering in the perovskite structure was explained in terms of structure, B-site cation ratio, and A-site cation size as well as charge and size balance of the B-site ions.[3]

In the structurally ordered state, Sc^{3+} and Ta^{5+} ions alternate in adjacent B-sites forming a rock-salt structure in the octahedral sublattice with effectively doubling the lattice parameter(s) of a primitive perovskite cell. Thus the x-ray diffraction (XRD) pattern is characterized by the appearance of superlattice reflections associated with half-integer spacing of the disordered structure. The ordered PST shows a sharp first-order phase transition between paraelectric and ferroelectric states.[2] In the disordered state, the two ions are distributed statistically in the B-site sublattice and PST behaves like a typical relaxor with diffuse phase transition (DPT) and lower Curie temperature.[2] The DPT behavior was frequently explained by the existence of microdomains due to compositional fluctuation.[4]

PST samples prepared by conventional ceramic processing are normally in the mixed state of ordering. The structure can be modified to a different state, i.e., the degree of ordering can be controlled with suitable thermal annealing.[3,6] In practice, totally disordered PST was reported,[5,6] but completely ordered samples have not been prepared yet.[7] Besides PST, other materials, including $Pb(Sc_{1/2}Nb_{1/2})O_3$,[3,5,6,8,9] $Pb(In_{1/2}Nb_{1/2})O_3$,[9-12] and $Pb(In_{1/2}Ta_{1/2})O_3$,[8,10] were also studied for the controllability of ordering/disordering by proper heat treatments. In another scheme, modification to obtain different domain size of ordered region was attempted by composition modification of $Pb(Mg_{1/3}Nb_{2/3})O_3$ (PMN).[13]

In this paper, the effect of composition change on phase formation and dielectric characteristics was investigated for PST, which is often selected for studying the ordering/disordering phenomenon by thermal means. The composition was modified through a partial change of the ratio between Sc^{3+} and Ta^{5+} ions by taking x = -1/24, 0, 1/24, 2/24, 3/24, and 4/24 for $Pb(Sc_{1/2-x}Ta_{1/2+x})O_{3+x}$.

II. Experimental

Overall experimental procedure is depicted as a block diagram in Fig. 1. The chemicals were > 99.9 % pure and weighed to meet the formulae listed in the composition column of Table 1. Raw chemicals were milled for 12 h in a polyethylene bottle, with ZrO_2 balls and isopropyl alcohol (IPA) as milling media and liquid, respectively. After milling and drying, direct (one-step) calcination was carried out at several steps from 875° to 1100°C for 2 h to ensure complete reaction. 12 h millings were introduced between each step for homogenization. Phases of the calcined powder were checked out by XRD (Cu target, Ni filter; 40 kV, 10 mA). After granulation with a 3 weight % aqueous solution of Carbowax as binder, pellets were formed uniaxially first and then isos-

tatically compacted further at a pressure of 140 MPa. For sintering, the pellets were fired in an inverted double-crucible setup, with lead atmosphere generated from the same composition powder placed around the pellet and $PbZrO_3$ powder around the inverted inner crucible rim to seal the atmosphere. The pellets were sintered at temperatures between 1400° and 1500°C for 2 h at a heating rate of 5°C/min, with a 1 h hold at 550°C for binder burnout. Fired pellets were polished with a 600-grit SiC paper followed by a 1 μm Al_2O_3 paste, cleaned ultrasonically, and were sputtered with gold on both sides as electrode. Dielectric constants and losses were measured at several frequencies ($10^{2\sim6}$ Hz) under a weak AC field of 1.0 V_{rms}/mm, using a precision LCR meter (HP-4284A), over a temperature range of -100° to 200°C on heating and cooling in a temperature chamber (Delta Design 9023).

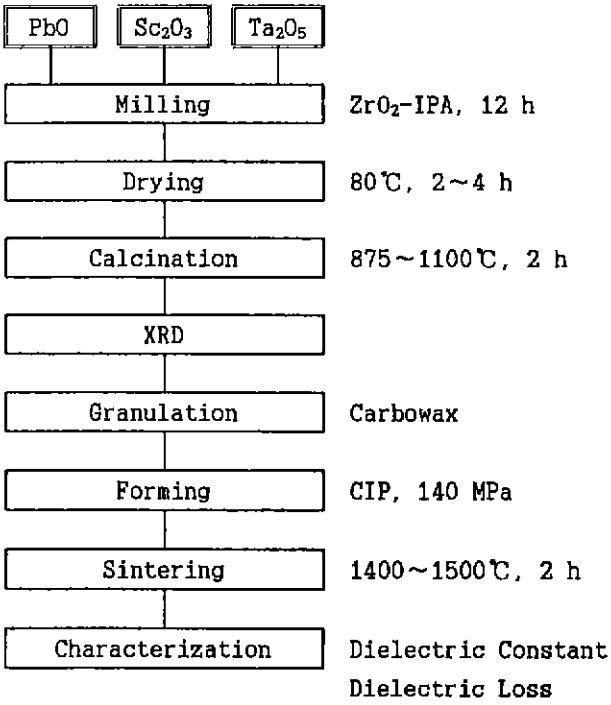

Fig. 1. Block diagram of the experimental procedure.

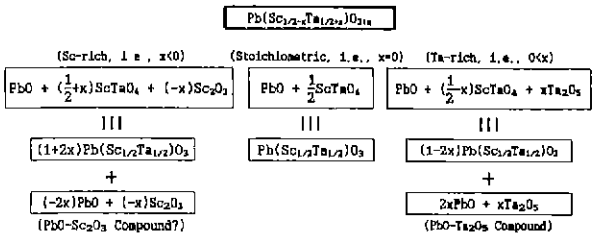

Fig. 2. Prediction of phase formation for $Pb(Sc_{1/2-x}Ta_{1/2+x})O_{3+x}$ composition.

III. Results and Discussion

Systematic predictions of phase formation for stoichiometric and nonstoichiometric (scandium-rich and tantalum-rich) compositions of PST series are presented in Fig. 2, from which the compositions in Table 1 were selected. For the scandium-rich case, unreacted Sc_2O_3, after forming perovskite phase, may/may not form compound(s) with PbO in the ratio as listed in Table 1. The formability, however, is uncertain since the phase diagram of $PbO\text{-}Sc_2O_3$ is not available. In the reverse case of tantalum-rich composition, excess Ta_2O_5 will react with leftover PbO to form $PbO\text{-}Ta_2O_5$ compound(s), as expected from the corresponding phase diagram.[14]

In Fig. 3 are the XRD charts of each composition after calcination. X-ray study showed that PST0 powder crystallized basically into a partially-ordered perovskite structure with small traces of $Pb_3Ta_4O_{13}$ (P_3T_2) pyrochlore phase. Fundamental lines corresponding to the perovskite structure are indexed based on a primitive unit cell and superstructure reflections with fractional indices are also included in Fig. 3. For PST-1, the pattern is quite similar to that of PST0 powder. The undetectability of excess PbO and Sc_2O_3 is currently interpreted as follows: they do not react to form compound(s) so free PbO was readily volatilized during the calcination of 875°~1100°C while free Sc_2O_3, though nonvolatile, could not be detected distinctly due to the low scattering factor of scandium ion. As tantalum content increased, the P_3T_2 phase developed further during the expense of perovskite, as expected from the prediction of Fig. 2 and Table 1. At higher tantalum contents, $Pb_5Ta_4O_{15}$(P_5T_2) was also developed. In the case of PST4 specimen, however, the major phase was P_3T_2, which is a tantalum analog of $Pb_3Nb_4O_{13}$ (P_3N_2). P_3N_2 is the notorious phase in the synthesis of lead-based complex perovskites containing niobium, $Pb(B_{1/3}Nb)O_3$.

Table 1. Symbol and Composition of $Pb(Sc_{1/2-x}Ta_{1/2+x})O_{3+x}$ Series.

x	Symbol	Composition	$Pb(Sc_{1/2}Ta_{1/2})O_3$	PbO	Sc_2O_3	Ta_2O_5
x < 0	PST-1	$Pb(Sc_{13/24}Ta_{11/24})O_{3+x}$	11/12	1/12	1/24	
x = 0	PST0	$Pb(Sc_{12/24}Ta_{12/24})O_3$	12/12			
0 < x	PST1	$Pb(Sc_{11/24}Ta_{13/24})O_{3+x}$	11/12	1/12		1/24
	PST2	$Pb(Sc_{10/24}Ta_{14/24})O_{3+x}$	10/12	2/12		2/24
	PST3	$Pb(Sc_{9/24}Ta_{15/24})O_{3+x}$	9/12	3/12		3/24
	PST4	$Pb(Sc_{8/24}Ta_{16/24})O_{3+x}$	8/12	4/12		4/24

By adopting the so-called two-step calcination, it may be possible to reduce/eliminate the trace pyrochlores persistent in preparing perovskite PST.

PST-1 specimen looked physically inhomogeneous with many specks after sintering, so was not examined any further. Based on the XRD intensity, long-range order parameters (S) were obtained using the following equation,

$$S^2 = \left(\frac{I_{1/2\ 1/2\ 1/2}}{I_{100}}\right)_{obs} / \left(\frac{I_{1/2\ 1/2\ 1/2}}{I_{100}}\right)_{calc\ S=1}$$

where the denominator is 1.33 for completely ordered PST (S=1). The order parameters are then 0.64 (PST-1), 0.70 (PST0), 0.78 (PST1), 0.62 (PST2), 0.60 (PST3), and 0.57 (PST4), with a trend of increasing to PST1 followed by a sharp decline. The abrupt change of the order parameter between PST1 and PST2 is not fully understood at the present time.

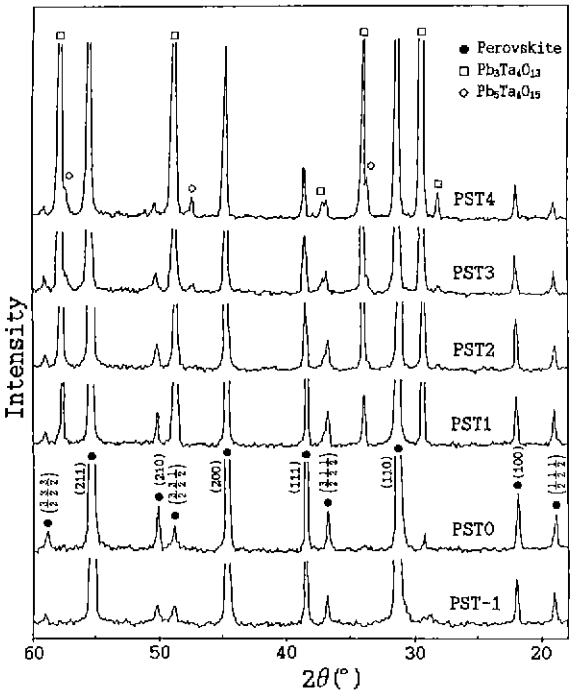

Fig. 3. XRD patterns of PST-series powder.

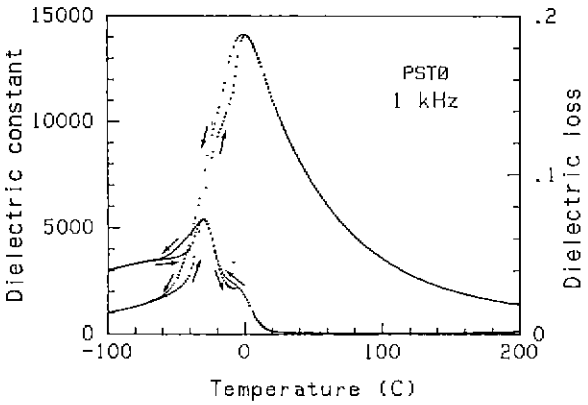

Fig. 4. Thermal hysteresis in dielectric constant and loss of PST0 specimen.

Fig. 4 shows two sets of curves, dielectric constant and dielectric loss, of PST0 specimen, measured at 1 kHz on cooling and heating (denoted by arrows). The dielectric constants followed the same trace in the paraelectric region, but the dielectric constants at ferroelectric region and dielectric losses at both region showed a certain degree of hysteresis. This kind of thermal hysteresis in the ferroelectric region was also reported for $Pb(Sc_{1/2}Nb_{1/2})O_3$[8] and $Pb(Co_{1/2}W_{1/2})O_3$[15] as well as PST crystal[2] and was explained to be originating from the first-order nature of the phase transition in the well-ordered sample. In contrast, the heating and cooling curves of PMN(T_C=-10°C) did not show any hysteresis in both region in the temperature range of -100°~200°C.[16]

For the dielectric constant, inflection is uncertain on cooling, but is pronounced in the case of the heating curve and is more pronounced in the dielectric losses. Considering the inflections, it seems that there are two or more phase transformation kinetic mechanisms competing in the ferroelectric region. For the rest of the study, only the cooling curves with a small degree of inflection will be shown.

Fig. 5 shows the temperature dependence of dielectric constants and losses of each specimen (except PST-1), measured at 100 Hz, 1, 10, and 100 kHz, and 1 MHz. Temperatures corresponding to the maximum values of dielectric constants and losses were relatively insensitive to the measuring frequency, i.e., all of the compositions showed a negligible shift of Curie temperatures with measuring frequency (ΔT_C=5°~7°C between 100 Hz and 1 MHz), which can be expected from the high order parameters (S=0.57~0.78). There is, however, a moderate suppression of the dielectric constant values with increasing frequency, e.g., maximum value of PST0 sample decreased from 14,600 (100 Hz) to 12,100 (1 MHz). At the same time, maximum dielectric loss increased from 7.0% to 12% in the same frequency range. Meanwhile the dielectric loss passed through a maximum at typically 25°~30°C lower than the Curie temperatures, which is common to relaxor ferroelectric materials. It is also worth noting that the inflections in the curves of dielectric constants and losses became less distinct as the frequency increased. The reason behind this change is not quite clear at the moment, but can also be considered to be related to the kinetic mechanisms.

The temperature dependence of dielectric constants (measured at 1 kHz) for each composition are replotted in Fig. 6 for comparison. The Curie temperatures were rather insensitive to the B-site cation ratio (actually decreased slightly, up to 3°C, with increase of the tantalum content), while the peak values were strongly suppressed from 14,100 (PST0) to 2,100 (PST4). This marked de-

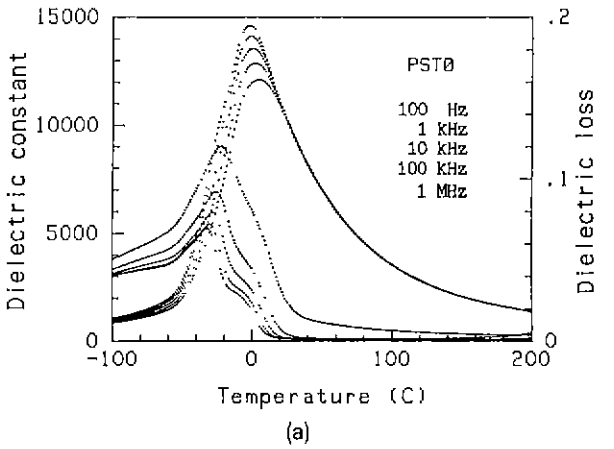

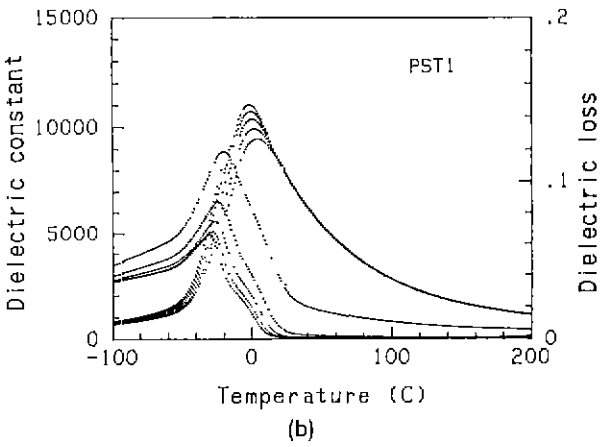

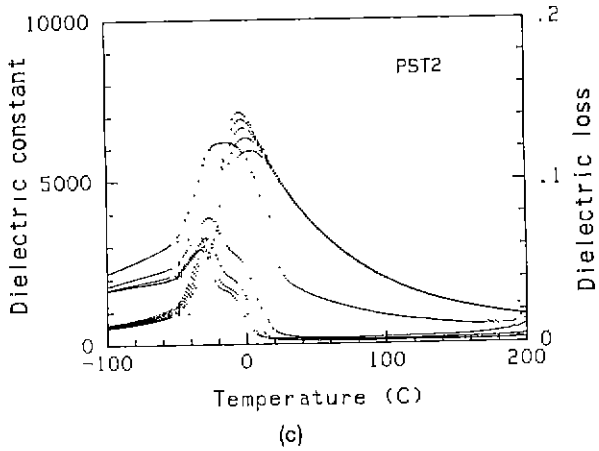

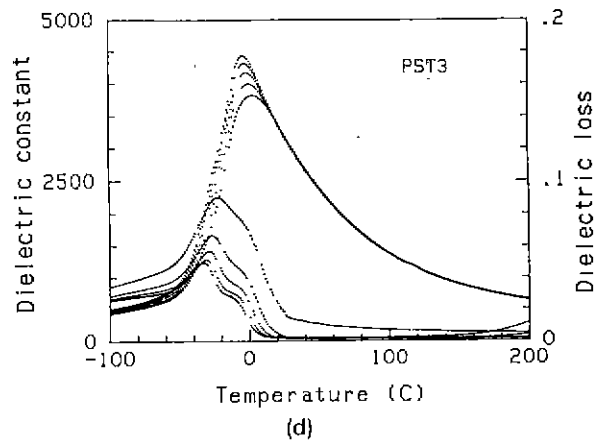

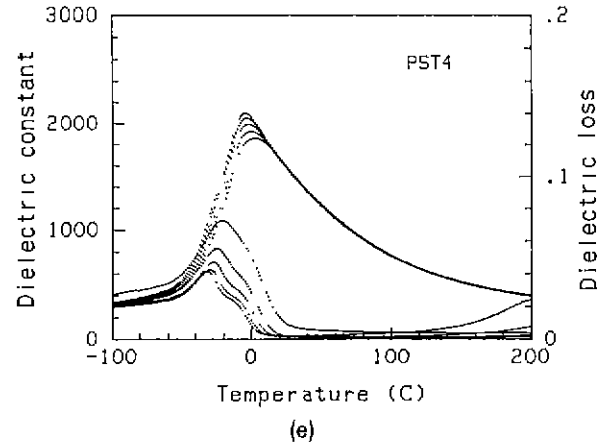

Fig. 5. Temperature dependence of dielectric constants and losses of PST-series specimen. (a) PST0, (b) PST1, (c) PST2, (d) PST3, and (e)PST4. Note the change of scale in vertical axis.

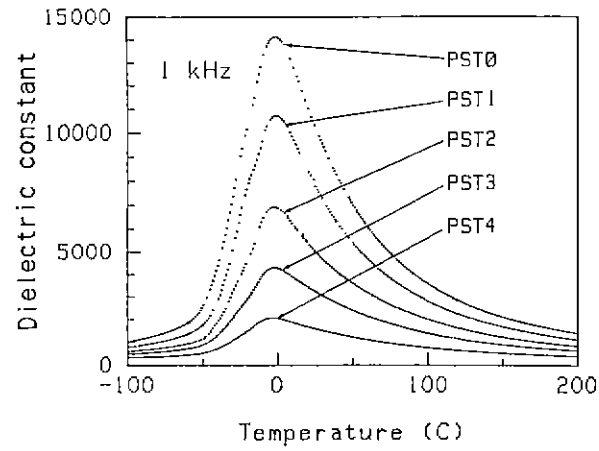

Fig. 6. Dielectric constant-temperature characteristics of PST-series specimen.

crease in the maximum dielectric constants can be explained by the dilution effect of the P_3T_2/P_5T_2 pyrochlore phases. The maximum value of dielectric constant, 14,100, of stoichiometric PST composition is quite high compared with the reported value,[1,17] while Curie temperature was -1°C and is somewhat lower than the reported data,[1,17-19] all of which may be ascribed to the different degree of ordering.

IV. Conclusion

Stoichiometric and nonstoichiometric (Sc-rich and Ta-rich) compositions of PST-series specimens were prepared and characterized. All of the calcined powders crystallized into a perovskite structure (order parameter=0.57~0.78) with increasing pyrochlore phases as the tantalum content increased. The prepared samples showed thermal hysteresis in dielectric properties and also showed a relaxor behavior with a negligible shift of Curie temperatures (ΔT_C=5°~7°C between 100 Hz and 1

MHz) while the maximum values were greatly influenced by the frequency. Curie temperatures were also insensitive to, while maximum dielectric constants were greatly suppressed by, the composition change.

Acknowledgments

This work was supported by US DOE and ONR, with a partial support for one of the authors (NKK) by Ministry of Education Research Fund for Advanced Materials in 1994

References

1. G. A. Smolenskii, V. A. Isupov and A. I. Agranovskaya, "New Ferroelectrics of Complex Composition of the Type $A^{2-}{}_2(B_I^{3+}B_{II}^{5-})O_6$. I," *Sov. Phys. -Solid State*, **1**[1], 150-51 (1959).
2. N. Setter and L. E. Cross, "The Role of B-Site Cation Disorder in Diffuse Phase Transition Behavior of Perovskite Ferroelectrics," *J. Appl. Phys.*, **51**[8], 4356-60 (1980).
3. N. Setter and L. E. Cross, "The Contribution of Structural Disorder to Diffuse Phase Transitions in Ferroelectrics," *J. Mater. Sci.*, **15**[10], 2478-82 (1980).
4. G. A. Smolenskii, "Physical Phenomena in Ferroelectrics with Diffused Phase Transition," *J. Phys. Soc. Jpn.*, **28**, Suppl. 26-37 (1970).
5. C. G. F. Stenger and A. J. Burggraaf, "Order-Disorder Reaction in the Ferroelectric Perovskites $Pb(Sc_{1/2}Nb_{1/2})O_3$ and $Pb(Sc_{1/2}Ta_{1/2})O_3$. I. Kinetics of the Ordering Process," *Phys. Status Solidi* (a), **61**[1], 275-85 (1980).
6. C. G. F. Stenger and A. J. Burggraaf, "Order-Disorder Reaction in the Ferroelectric Perovskites $Pb(Sc_{1/2}Nb_{1/2})O_3$ and $Pb(Sc_{1/2}Ta_{1/2})O_3$. II. Relation between Ordering and Properties," *Phys. Status Solidi* (a), **61**[2], 653-64 (1980).
7. N. Setter and L. E. Cross, "Pressure Dependence of the Dielectric Properties of $Pb(Sc_{1/2}Ta_{1/2})O_3$," *Phys. Status Solidi* (a), **61**[1], K71-75 (1980).
8. A. Kania and M. Pawelczyk, "Order-Disorder Aspects in $PbIn_{0.5}Ta_{0.5}O_3$ Crystals," *Ferroelectrics*, **124**, 261-64 (1991).
9. A. Kania and E. Rowinski, "Dielectric Properties for Differently Quenched $PbIn_{0.5}Nb_{0.5}O_3$ Crystals," *Ferroelectrics*, **124**, 265-70 (1991).
10. N. Yasuda, H. Inagaki and S. Imamura, "Dielectric Properties of Perovskite Lead Indium Niobate and Tantalate Prepared by Fast Firing Technique," *Jpn. J. Appl. Phys.*, **31**Part2[5A], L574-75 (1992).
11. N. Yasuda and M. Fujie, "Dielectric Properties of Lead-Based Complex Perovskite Solid Solution $Pb(In_{1-x/2}Yb_{x/2}Nb_{1/2})O_3$," *Jpn. J. Appl. Phys.*, **31**[9B], 3128-31 (1992).
12. J. Ravez, F. Weill and C. Elissalde, "$Pb(In_{1/2}Nb_{1/2})O_3$ Ceramic: Preparation and Nanostructural Studies," Proc. 4th Int. Conf. Electroceramics & Appl., pp. 455-58 (1994).
13. J. Chen, H. M. Chan and M. P. Harmer, "Ordering Structure and Dielectic Properties of Undoped and La/Na-Doped $Pb(Mg_{1/3}Nb_{2/3})O_3$," *J. Am. Ceram. Soc.*, **72**[4], 593-98 (1989).
14. E. M. Levin, C. R. Robbins and H. F. McMurie, Phase Diagrams for Ceramists, **1**, Fig. 289, The American Ceramic Society, 1964.
15. V. A. Bokov, S. A. Kizhaev, I. E. Myl'nikova and A. G. Tutov, "Antiferroelectric and Magnetic Properties of $PbCo_{1/2}W_{1/2}O_3$," *Sov. Phys.-Solid State*, **6**[10], 2419-24 (1965).
16. unpublished work.
17. Y. Yamashita, "PZN-Based Relaxors for MLCCs," *Am. Ceram. Soc. Bull.*, **73**[8], 74-80 (1994).
18. N. Setter and L. E. Cross, "Flux Growth of Lead Scandium Tantalate $Pb(Sc_{1/2}Ta_{1/2})O_3$ and Lead Magnesium Niobate $Pb(Mg_{1/3}Nb_{2/3})O_3$ Single Crystals," *J. Crystal Growth*, **50**[2], 555-56 (1980).
19. X.-W. Zhang, Q. Wang and B. L. Gu "Study of the Order-Disorder Transition in $A(B'B'')O_3$ Perovskite Type Ceramics," *J. Am. Ceram. Soc.*, **74**[11], 2846-50 (1991).